Fusogen-mediated neuron–neuron fusion disrupts neural circuit connectivity and alters animal behavior

Rosina Giordano-Santini[a], Eva Kaulich[a], Kate M. Galbraith[a,1], Fiona K. Ritchie[a,1], Wei Wang[b,1], Zhaoyu Li[b], and Massimo A. Hilliard[a,2]

[a]Clem Jones Centre for Ageing Dementia Research, Queensland Brain Institute, The University of Queensland, Brisbane, QLD 4072, Australia; and [b]Queensland Brain Institute, The University of Queensland, Brisbane, QLD 4072, Australia

Edited by Yishi Jin, University of California San Diego, La Jolla, CA, and accepted by Editorial Board Member Yuh Nung Jan July 24, 2020 (received for review November 3, 2019)

The 100-y-old neuron doctrine from Ramón y Cajal states that neurons are individual cells, rejecting the process of cell–cell fusion in the normal development and function of the nervous system. However, fusogens—specialized molecules essential and sufficient for the fusion of cells—are expressed in the nervous system of different species under conditions of viral infection, stress, or disease. Despite these findings, whether the expression of fusogens in neurons leads to cell–cell fusion, and, if so, whether this affects neuronal fate, function, and animal behavior, has not been explored. Here, using *Caenorhabditis elegans* chemosensory neurons as a model system, we provide proof-of-principle that aberrant expression of fusogens in neurons results in neuron–neuron fusion and behavioral impairments. We demonstrate that fusion between chemoattractive neurons does not affect the response to odorants, whereas fusion between chemoattractive and chemorepulsive neurons compromises chemosensation. Moreover, we provide evidence that fused neurons are viable and retain their original specific neuronal fate markers. Finally, analysis of calcium transients reveals that fused neurons become electrically coupled, thereby compromising neural circuit connectivity. Thus, we propose that aberrant expression of fusogens in the nervous system disrupts neuronal individuality, which, in turn, leads to a change in neural circuit connectivity and disruption of normal behavior. Our results expose a previously uncharacterized basis of circuit malfunction, and a possible underlying cause of neurological diseases.

neuronal fusion | fusogen | *C. elegans* | cell–cell fusion | chemosensation

Our view of modern neuroscience is based upon the neuron doctrine of Ramón y Cajal, which defines neurons as individual cells. Although gap junctions allow sharing of small signaling molecules and electrical coupling between neurons (1), no membrane or full cytoplasmic continuity exists between these cells (2), excluding the process of cell–cell fusion during normal development and function of the nervous system. However, fusogens, specialized proteins responsible for merging the plasma membranes of fusing cells, are expressed in the nervous system of invertebrates and vertebrates under specific stress conditions (3). In humans, Syncytin-1, which is responsible for fusing thousands of epithelial cells to form the syncytiotrophoblast layer of the placenta, is expressed in the brain of patients with multiple sclerosis (4). In mice, pseudorabies virus glycoprotein B, which is required for the fusion of the viral envelope with the cellular membrane during viral cell entry, has been associated with abnormal cell–cell fusion of infected parasympathetic neurons (5). In *Caenorhabditis elegans*, Epithelial Fusion Failure-1 (EFF-1) and Anchor cell Fusion Failure-1 (AFF-1), which mediate developmental fusion in several tissues, are expressed in neurons and glia (6, 7). EFF-1 is involved in the remodeling of dendritic trees (8, 9) and axonal regeneration by fusion (10, 11), whereas AFF-1 has been shown to mediate dendritic regeneration by fusion (9, 12) and glial cell–cell fusion (13). Moreover, EFF-1 has been associated with the abnormal cell–cell fusion of *C. elegans* neurons during axonal regeneration (11). These discoveries expose an important aspect of the nervous system that has remained largely unexplored: the presence of fusogens can lead to abnormal neuronal fusion, placing these cells at risk of losing their individuality. However, our knowledge of the functional consequences of neuronal fusion is very limited (5, 14, 15), and whether aberrant expression of fusogens in neurons is sufficient to induce their fusion, and how this affects connectivity and behavior, is not known.

The complexity of the vertebrate nervous system has hindered the study of this problem. Inducing and visualizing neuronal fusion in a vertebrate brain with billions of highly arborized neurons, and linking these fusion events to specific behaviors, is technically challenging. The nematode *C. elegans* provides a useful model in this regard, as it is possible to pair the function of single neurons with distinct behavioral outputs (16). The 302 neurons of the adult hermaphrodite have an invariable morphology and position (17), and their contacts have been identified in a complete wiring diagram of the nervous system (18). Moreover, the genetic amenability of *C. elegans* and the availability of well-characterized fusogens (6, 7) make it possible to manipulate the expression of fusogens at the level of single neurons.

We focused on two bilaterally symmetric pairs of chemosensory neurons in the head of the animal: Amphid Wing C (AWC) left and right, and Amphid Wing B (AWB) left and right (Fig. 1*A*). These two pairs of cells have a simple morphology,

Significance

Ramón y Cajal's neuron doctrine, which states that neurons are individual cells that do not share any membrane or cytoplasmic continuity between them, has underpinned our view of modern neuroscience. However, there is considerable evidence that fusogens, specialized proteins essential and sufficient for the fusion of cells in other tissues, are expressed in the nervous system of several species in response to viral infection, stress conditions, and neurological disease. By manipulating the expression of fusogens in the chemosensory neurons of *Caenorhabditis elegans*, our results provide conclusive evidence that deregulation of fusogen expression causes neuronal fusion and can have deleterious effects on neural circuitry and behavioral outputs, revealing a possible novel underlying cause of neurological disorders.

Author contributions: R.G.-S., Z.L., and M.A.H. designed research; R.G.-S., E.K., K.M.G., F.K.R., and W.W. performed research; R.G.-S., E.K., K.M.G., F.K.R., W.W., Z.L., and M.A.H. analyzed data; and R.G.-S. and M.A.H. wrote the paper.

The authors declare no competing interest.

This article is a PNAS Direct Submission. Y.J. is a guest editor invited by the Editorial Board.

[1]K.M.G., F.K.R., and W.W. contributed equally to this work.

[2]To whom correspondence may be addressed. Email: m.hilliard@uq.edu.au.

This article contains supporting information online at https://www.pnas.org/lookup/suppl/doi:10.1073/pnas.1919063117/-/DCSupplemental.

First published August 27, 2020.

their function correlates with specific chemosensory responses, and their axons and dendrites are tightly associated, providing putative fusion sites. Their cell bodies are located on each side of the pharynx, and each neuron extends a single axon that enters the nerve ring, as well as a single dendrite to the tip of the nose that terminates with a specialized cilium (Fig. 1*A*). The tightly associated axons of the two AWC neurons form reciprocal synapses in the nerve ring, whereas the two AWB neurons communicate with each other through gap junctions located at the end of their respective axons (18). Both AWC neurons are responsible for the chemoattraction response to a source of odorant, but, despite their identical morphology, they have different cell identities (AWC^{ON} and AWC^{OFF}), defined by the specific genes that they express and the odorants they detect (19–23). In contrast, the AWB neurons are responsible for the detection of repellent stimuli (24).

Here we demonstrate that misexpression of the nematode fusogen EFF-1 in these *C. elegans* chemosensory neurons leads to neuronal fusion. We show that fused neurons mix their diffusible cytoplasmic content but retain the expression of their original cell fate-specific markers. Furthermore, we reveal that fusion between the two chemoattractive AWC^{ON} and AWC^{OFF} neurons does not affect chemoattraction, whereas fusion of a chemoattractive AWC neuron with the chemorepulsive AWB neurons results in impaired chemosensation. Using mutant animals with defects in specific neuronal compartments, we also demonstrate that fusion selectively occurs at the level of the axons. Finally, analysis of calcium transients upon neuronal activation suggests that the impaired chemosensory behavior is due to the simultaneous activation of the chemoattraction and chemorepulsion neuronal circuits.

Results

Misexpression of Fusogens in Neurons Leads to Neuronal Cell–Cell Fusion. We first asked whether misexpression of fusogens in neurons could lead to neuronal fusion. We used the nematode fusogen EFF-1, which has been shown to be required on both partner cells to mediate fusion in other *C. elegans* tissues (6, 25), and selectively expressed it in the AWC^{ON} and AWC^{OFF} neurons of transgenic animals expressing a cytoplasmic red fluorophore in AWC^{ON}, and a cytoplasmic green fluorophore in AWC^{OFF} (*Pstr-2::DsRed; Psrsx-3::GFP*). We reasoned that, if fusion were to occur between these cells, it would result in the diffusion and mixing of the two fluorophores in both AWC neurons (Fig. 1*A*). Indeed, mixing of fluorophores occurred when EFF-1 was expressed in both cells (*Podr-1::eff-1* or *Pstr-2::eff-1; Psrsx-3::eff-1*), but only to a minimal extent when EFF-1 was expressed in only one AWC neuron (*Pstr-2::eff-1* or *Psrsx-3::eff-1*) (Fig. 1 *B–D*). This phenotype was not caused by an excess of the AWC promoters used to drive the expression of the fusogens, as transgenes with the promoters alone did not cause fluorophore mixing (Fig. 1*D*). Moreover, expression of EFF-1 under a heat shock promoter (*Phsp-16.2::eff-1*) (26) led to mixing of fluorophores only following heat shock, suggesting that this phenotype is specific to the expression of EFF-1 (*SI Appendix*, Fig. S1). We also found that mixing of fluorophores did not occur when we expressed a nonfusogenic form of EFF-1 (*Podr-1::EFF-1(T173A/N529D)*) (27), demonstrating that it is the fusogenic capacity of EFF-1 which enables this phenotype (Fig. 1*D*). Finally, expression of AFF-1, which has also been shown to be required on both partner cells to mediate fusion in other *C. elegans* tissues (7, 28), also caused mixing of fluorophores between AWC^{ON} and AWC^{OFF} when simultaneously expressed in these neurons (*Podr-1::aff-1*) (Fig. 1*D*).

To confirm that the mixing of fluorophores between AWC^{ON} and AWC^{OFF} was due to a true fusion event, we used the photoconvertible protein Kaede, a fluorophore that can be irreversibly converted from green to red using ultraviolet light (29, 30) (Fig. 1*E*). We expressed Kaede only in AWC^{ON} (*Pstr-2::Kaede*), together with EFF-1 in both AWC neurons (*Podr-1::eff-1*). This resulted in animals in which Kaede was present in both AWC cells. Next, we converted Kaede in only one AWC neuron, and monitored its diffusion to the contralateral neuron. Converted Kaede was detected in the contralateral neuron immediately following conversion, and the intensity increased significantly over a period of 30 min (Fig. 1*F*). Importantly, this phenomenon was not observed when the same *Pstr-2::Kaede* transgene was expressed in *nsy-1* mutant animals in which both AWC neurons acquire an AWC^{ON} fate (31) (Fig. 1 *E* and *G*). In these animals, conversion of Kaede in only one AWC neuron did not result in the appearance of converted Kaede in the contralateral AWC neuron (Fig. 1*G*), as expected from individual cells with unconnected cytoplasms. These results confirm that expression of EFF-1 in both AWC neurons results in fusion pores and diffusion of cytoplasmic fluorophores between the two neurons. They are also consistent with previous work showing that ectopic expression of EFF-1 in heterologous cells leads to membrane fusion and cytoplasmic mixing (32, 33). Importantly, because Kaede is a 116-kDa tetrameric protein unable to diffuse through gap junctions (29, 30), these results set a lower limit on the size of the fusion pores generated by EFF-1 in neurons.

We next asked whether this fusion capacity was unique to the AWC chemosensory neurons, or whether other neurons could also fuse following misexpression of fusogens. Using the diffusion of cytoplasmic fluorophores between cells as a readout of cell–cell fusion, we observed fusion between the attractive AWC^{ON} neuron and the two repulsive AWB neurons following overexpression of EFF-1 in these cells (*Pstr-2::eff-1; Pstr-1::eff-1*) (Fig. 2 *A–C* and *G*). In some animals, we also observed diffusion of the cytoplasmic fluorophores to the ASI neurons, another pair of chemosensory neurons that form synapses with the AWC neurons (18), and in which the AWC^{ON} promoter used for the expression of EFF-1 (*Pstr-2*) is also active (*SI Appendix*, Fig. S2). This suggested that the AWC^{ON} and AWB neurons had also fused with ASI, forming a syncytium composed of up to five cells. Following a similar strategy, we also observed fusion between the attractive AWC^{OFF} and the repulsive AWB neurons when EFF-1 was expressed in these three cells (*Psrsx-3::eff-1*) (Fig. 2 *D–F* and *H*). Next, we asked whether other classes of neurons could also undergo cell–cell fusion following overexpression of fusogens. We found that the PLM mechanosensory neuron and the PLN oxygen-sensing neuron, whose axons fasciculate along their trajectory from the tail toward the midbody of the animal, also underwent fusion upon simultaneous expression of EFF-1 (*Pmec-4::eff-1; Plad-2::eff-1*) (*SI Appendix*, Fig. S3).

Finally, we asked whether cell–cell fusion could also take place between neurons and glia. The Amphid sheath (AMsh) cells are located on the dorsal side of the pharynx terminal bulb and extend a thick process to the tip of the nose that encloses the amphid neurons' dendrites and cilia (*SI Appendix*, Fig. S4*A*). We therefore overexpressed AFF-1 in these cells and in the AWC and AWB amphid neurons (*PF16F9.3::aff-1; Podr-1::aff-1*), together with a cytoplasmic red fluorophore in AMsh, and a cytoplasmic green fluorophore in AWC and AWB neurons (*PF16F9.3::DsRed; Podr-1::GFP*). This resulted in mixing of fluorophores between AMsh and one or more of the amphid neurons in adult animals (*SI Appendix*, Fig. S4 *B–D*), as well as in dauer animals (*SI Appendix*, Fig. S4 *B*, *E*, and *F*), in which the right and left AMsh cells undergo remodeling followed by AFF-1-mediated cell–cell fusion at the tip of the nose (13, 34). Taken together, these experiments demonstrate that misexpression of fusogens in different sets of *C. elegans* neurons and glia is sufficient to induce neuron–neuron and neuron–glia fusion.

Fused Neurons Retain Expression and Localization of Their Original Cell Fate Markers. Cell–cell fusion can result in the reprogramming of a cell's fate following cytoplasmic mixing of specific factors between

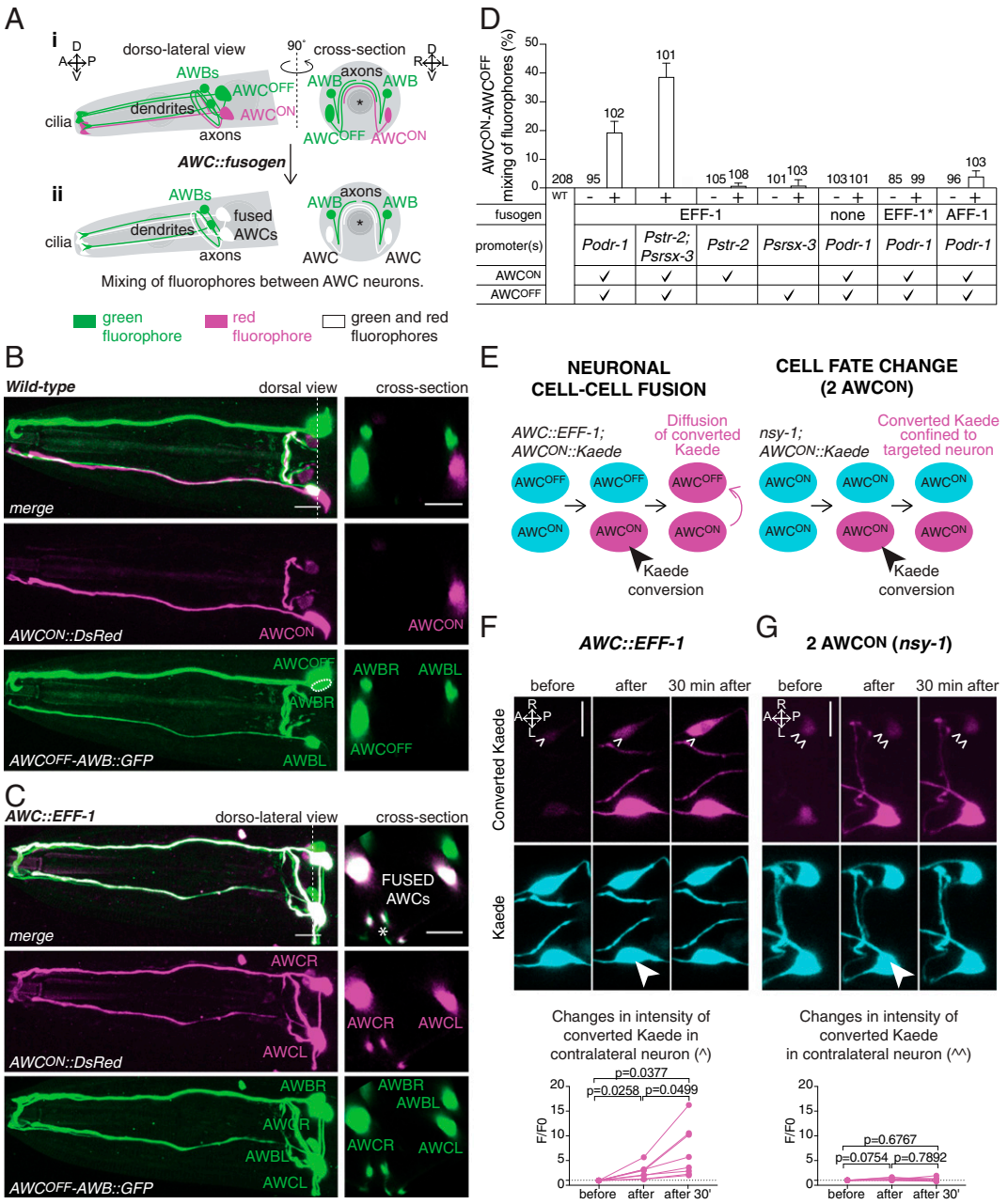

Fig. 1. Misexpression of fusogens in AWC chemosensory neurons results in neuronal cell–cell fusion. (*A*) Scheme of the AWC^{ON}, AWC^{OFF}, and AWB chemosensory neurons and the fusion assay. (*i*) In a wild-type animal, the attractive AWC^{OFF} neuron and the repulsive AWB neurons express a cytoplasmic green fluorophore (*Psrsx-3::GFP*), whereas the attractive AWC^{ON} neuron expresses a cytoplasmic red fluorophore (*Pstr-2::DsRed*). These neurons are in close contact at the level of their axons, a site of putative cell–cell fusion. (*ii*) Expression of fusogens in both AWC neurons (*AWC::fusogen*) results in the mixing of red and green fluorophores between AWC^{ON} and AWC^{OFF}, resulting in two green and red neurons. Asterisk represents the pharynx. A, anterior; P, posterior; D, dorsal; V, ventral; L, left; and R, right. (*B* and *C*) (*Left*) Confocal maximum z-projection images of the head of a wild-type animal (*B*), and an animal with fused AWC^{ON}–AWC^{OFF} (*C*). (*Right*) Cross-sections at the level of the cell bodies (indicated by a dotted line on the dorsal/dorso-lateral views). (Scale bars, 10 μm.) Asterisk in *C* shows a cross-section of the axons. (*D*) Quantification of AWC^{ON}–AWC^{OFF} mixing of fluorophore events in 1-d-old adult animals expressing either EFF-1, AFF-1, nonfusogenic EFF-1(T173A/N529D) (EFF-1*), or the promoter alone, in both AWC neurons, in AWC^{ON} only, or in AWC^{OFF} only. Mixing of fluorophores occurs when fusogens are concurrently expressed in both AWC neurons, either by expressing the fusogen under *Podr-1* or concurrently under *Pstr-2* and *Psrsx-3* promoters. The table on the *x* axis summarizes the fusogen expressed, the promoter used, and the neurons in which each promoter is active. "+" indicates transgenic animals, and "−" indicates nontransgenic siblings. WT, wild-type. Results are representative of at least two independent transgenic strains. N values are indicated in the graph. Error bars represent the SE of proportion. (*E*) Scheme of the assay used to determine cell–cell fusion using the photoconvertible protein Kaede. (*Left*) After conversion of Kaede in only one AWC neuron, diffusion to the contralateral neuron shows that the cytoplasms of the two neurons are connected, confirming that these cells have undergone cell–cell fusion. (*Right*) In cell fate mutant animals with two AWC^{ON} neurons (*nsy-1*), converted Kaede does not diffuse to the contralateral neuron. (*F* and *G*) (*Top*) Representative confocal sum z-projection images of the two AWC neurons of an animal expressing AWC::EFF-1 (*F*), and a *nsy-1* mutant animal with two AWC^{ON} neurons (*G*), before, immediately after, and 30 min after Kaede conversion in the neuron marked with a filled arrowhead. Converted Kaede diffuses to the contralateral neuron in animals expressing AWC::EFF-1, but not in animals with two AWC^{ON} neurons. (Scale bars, 10 μm.) (*F* and *G*) (*Bottom*) Quantification of the changes of converted Kaede in the contralateral neuron of AWC::EFF-1 animals (*F*), and *nsy-1* mutant animals (*G*). Comparisons between groups were obtained using the one-way ANOVA.

fused cells (35–37). Moreover, several cytoplasmic and transcription factors have been shown to determine the specific fate of chemosensory neurons. For instance, the lack of cytoplasmic or transcription factors involved in the determination and/or maintenance of the AWC^{ON} and AWC^{OFF} fates results in animals presenting either two AWC^{ON} or two AWC^{OFF} neurons (22, 23, 31, 38). Similarly, in the absence of the LIM-4 transcription factor, AWB neurons acquire an AWC^{ON} fate, whereas expression of LIM-4 in AWC^{ON} turns this cell into an AWB neuron (39). We therefore asked whether fusion between chemosensory neurons could lead to a cell fate change. We first analyzed the expression of specific markers in fused AWC^{ON}–AWC^{OFF} neurons. The AWC^{ON} and AWC^{OFF} fates have been extensively characterized, revealing genes expressed exclusively in either AWC^{ON} or AWC^{OFF} (21, 23, 38, 40). Given that the *str-2* gene is selectively expressed in AWC^{ON}, we used the *str-2* promoter to drive simultaneous expression of a cytoplasmic green fluorophore (GFP) and a nuclear red fluorophore (NLS::TagRFP) in this cell. Concurrently, we expressed the fusogen EFF-1 in both AWC neurons to induce fusion. We reasoned that neuronal fusion would allow the diffusion of cytoplasmic GFP from AWC^{ON} to AWC^{OFF}, whereas NLS::TagRFP would only appear in the contralateral AWC nucleus if this neuron had acquired an AWC^{ON} fate. As a positive control for neuronal cell fate change, we used *nsy-1* mutant animals, which have a two AWC^{ON} phenotype (31); as expected, these animals expressed GFP and NLS::TagRFP in both AWC neurons (Fig. 3*A*). However, animals with fused AWC^{ON}–AWC^{OFF} neurons, as evidenced by the diffusion of GFP between these cells, only expressed NLS::TagRFP in the AWC^{ON} neuron (Fig. 3*A*). Given that reprogramming to a new cell fate could take longer than the passive diffusion of a cytoplasmic fluorophore following cell–cell fusion, we analyzed 1-, 2-, and 3-d-old adults (1DOA, 2DOA, and 3DOA, respectively) for the expression of NLS::TagRFP in the contralateral neuron. We did not detect NLS::TagRFP expression in the fused contralateral AWC neuron in these three groups (*SI Appendix*, Fig. S5*A*), suggesting that AWC^{ON}–AWC^{OFF} fusion does not result in the acquisition of the ON fate by the AWC^{OFF} neuron. Given that the NLS::TagRFP expression did not turn off in AWC^{ON}, we also concluded that AWC^{ON}–AWC^{OFF} fusion does not result in the loss of the ON fate by the AWC^{ON} neuron.

We then applied a similar protocol to study the fate of the AWC and AWB neurons following fusion. We expressed GFP and NLS::TagRFP in AWC^{ON} neurons, and analyzed the expression of these markers in *lim-4* mutant animals where AWB cells acquire an AWC^{ON} fate (39), and in animals expressing EFF-1 in AWC^{ON} and AWB neurons. Whereas *lim-4* mutant animals expressed GFP and NLS::TagRFP in AWC^{ON} and the two AWB neurons, animals with fused neurons, as evidenced by the diffusion of GFP from AWC^{ON} to the AWB neurons, only expressed NLS::TagRFP in the AWC^{ON} neuron (Fig. 3*B*). This expression pattern was observed in 1DOA, 2DOA, and 3DOA (*SI Appendix*, Fig. S5*B*), suggesting that the AWB neurons do not acquire the AWC^{ON} fate following fusion. Because the NLS::TagRFP marker was not turned off in AWC^{ON}, these results also demonstrate that the AWC^{ON} neuron does not acquire an AWB fate following fusion. Alternatively, it is possible that the nuclei of the AWC^{ON}–AWC^{OFF} and AWC^{ON}–AWB neuronal syncytia remain distinct despite sharing a common cytoplasm with mixed identity, as has previously been observed in some syncytial organs of *C. elegans*, *Drosophila*, and vertebrates (41, 42).

To further explore cell fate following fusion, we investigated the expression and localization of an AWC^{ON}-specific G protein-coupled receptor (GPCR) on the chemosensory cilia of fused AWC^{ON} and AWB neurons. We expressed a red cytoplasmic protein (mCherry) in the AWB neurons, and a GFP-tagged version of the GPCR STR-2 (STR-2::GFP) in the AWC^{ON} neuron (*SI Appendix*, Fig. S6*A*). As expected, *lim-4* mutant animals in which the AWB neurons had acquired an AWC^{ON} fate failed to express mCherry in these cells, but presented STR-2::GFP on the cilia of AWC^{ON} and both AWB neurons. In contrast, animals with fused neurons, as evidenced by the diffusion of mCherry from AWB to AWC^{ON}, only presented STR-2::GFP in the cilium of the AWC^{ON} neuron (*SI Appendix*, Fig. S6 *B* and *C*). These findings suggest that the AWC–AWB fused neurons retain the expression and localization of their original GPCR-type olfactory receptors. In a similar experiment, we also found that AWC^{ON}–AWC^{OFF} fusion does not alter the expression and localization of the SRSX-3 AWC^{OFF}-specific odorant receptor, which remains present only in the cilium of the AWC^{OFF} neuron (*SI Appendix*, Fig. S7). Together, our results demonstrate that neuronal fusion does not alter the expression and localization of cell fate-specific markers, indicating that fused chemosensory neurons retain their original fate.

Fusion Between Neurons of Different Modalities Alters Behavior. We next hypothesized that loss of neuronal individuality caused by fusion would compromise the normal function of the neuron and/or the connectivity of neural circuits, resulting in an altered behavior. To test this hypothesis, we first investigated the chemoattractive response to butanone in animals with fused AWC^{ON} and AWC^{OFF} neurons. Butanone is detected exclusively by the AWC^{ON} neuron, and when this neuron is ablated the animal is no longer attracted to this odorant (19, 20) (Fig. 4*A*). We therefore performed chemosensory assays with individual animals that had undergone EFF-1–mediated fusion of AWC^{ON} and AWC^{OFF} neurons (*Podr-1::eff-1*). To avoid confounding results, we selected animals with specific AWC^{ON}–AWC^{OFF} fusion, and excluded animals in which the AWC^{ON} and AWC^{OFF} neurons had also fused with other neurons (*SI Appendix*, *Text*). As controls, we used wild-type animals as well as transgenic animals carrying an empty vector (*Podr-1::(empty)*), to account for any possible effect of transgenic markers and excess of the promoter element. Our results revealed that animals with fused AWC neurons were attracted to butanone, suggesting that fusion did not affect the function of AWC^{ON} (Fig. 4*B*). Similarly, we tested these animals for their chemoattraction to pentanedione, an odorant exclusively sensed by the AWC^{OFF} neuron (20) (Fig. 4*A*), and found no difference between animals with fused neurons and the wild-type or transgenic controls (Fig. 4*C*). Not surprisingly, these animals were also able to detect benzaldehyde, an odorant sensed by both AWC neurons (19) (Fig. 4 *A* and *D*). These results reveal that fused AWC^{ON} and AWC^{OFF} neurons are functional, and that fusion between these chemoattractive neurons does not alter the response to odorants detected specifically by these cells.

Next, we asked whether odorant discrimination, an ability that requires the distinct asymmetric fate of AWC^{ON} and AWC^{OFF} neurons (20), was affected in animals in which these neurons had undergone fusion. Wild-type animals with functional AWC^{ON} and AWC^{OFF} neurons discriminate between butanone (detected only by the AWC^{ON} neuron) and benzaldehyde (detected by both AWC neurons); constant exposure to butanone saturates the response of AWC^{ON}, but the animals are still able to detect benzaldehyde with the unaffected AWC^{OFF} neuron. This ability is lost in animals in which AWC^{OFF} has been ablated (only one AWC^{ON} neuron left), as well as in *nsy-1* mutant animals, which present loss of AWC asymmetry (two AWC^{ON} neurons) (20). Surprisingly, unlike *nsy-1* mutant animals, we found that animals with fused AWC^{ON}–AWC^{OFF} neurons were still able to discriminate between these odorants (*SI Appendix*, Fig. S8). These results demonstrate that fused AWC^{ON}–AWC^{OFF} neurons retain their discriminative capacity, and confirm our previous finding that AWC^{ON}–AWC^{OFF} fused neurons preserve their original cell fate asymmetry. Together with our previous behavioral results, these

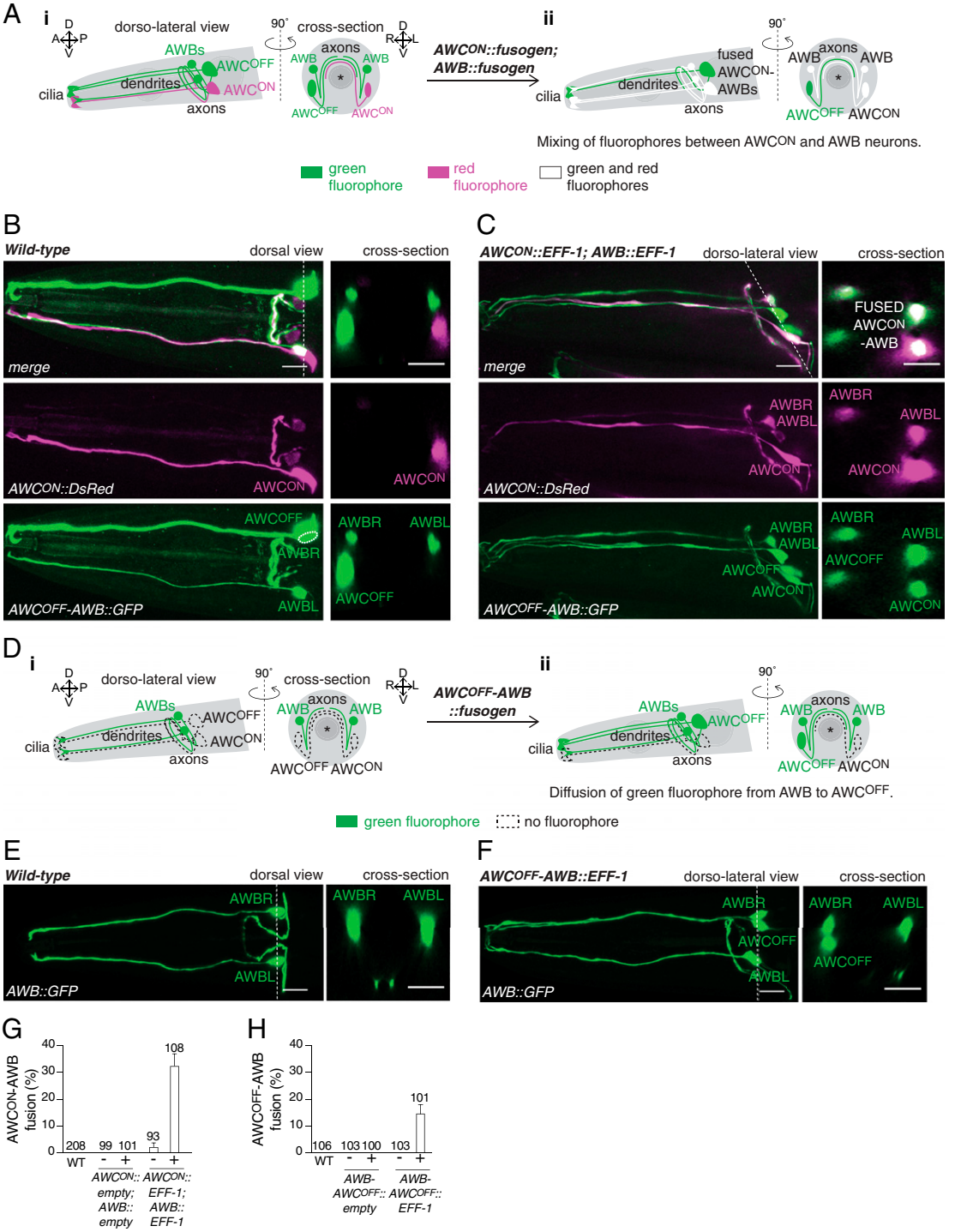

Fig. 2. Misexpression of fusogens leads to cell–cell fusion between attractive and repulsive chemosensory neurons. (*A*) Scheme of the AWC^{ON}, AWC^{OFF}, and AWB chemosensory neurons, and the fusion of the attractive AWC^{ON} with the repulsive AWB neurons. (*i*) In a wild-type animal, AWB neurons express a cytoplasmic green fluorohore (*Psrsx-3::GFP*), whereas the AWC^{ON} neuron expresses a cytoplasmic red fluorophore (*Pstr-2::DsRed*). (*ii*) Concurrent expression of fusogens in AWC^{ON} and AWB neurons (*AWC^{ON}::fusogen; AWB::fusogen*) results in the mixing of red and green fluorophores between these neurons. Asterisk represents the pharynx. (*B* and *C*) (*Left*) Representative confocal maximum z-projection images of the head of a wild-type animal (*B*), and an animal with AWC^{ON}–AWB fusion (*C*). (*Right*) Cross-sections at the level of the cell bodies (indicated by a dotted line on the dorsal/dorso-lateral views). Image in *B* is the same as shown in Fig. 1*B*. (Scale bars, 10 μm.) (*D*) Scheme of the attractive AWC^{OFF} and the repulsive AWB chemosensory neurons, and fusion of these cells. (*i*) In a wild-type animal, AWB neurons express a cytoplasmic green fluorophore (*Pstr-1::GFP*). (*ii*) Concurrent expression of fusogens in AWC^{OFF} and AWB neurons (*AWC^{OFF}–AWB::fusogen*) results in diffusion of the green fluorophore from AWB to the AWC^{OFF} neuron. Asterisk represents the pharynx. (*E* and *F*) (*Left*) Representative confocal maximum z-projection images of the head of a wild-type animal (*E*), and an animal with AWC^{OFF}–AWB fusion (*F*). (*Right*) Cross-sections at the level of the cell bodies (indicated by a dotted line on the dorsal/dorso-lateral views). (Scale bars, 10 μm.) (*G* and *H*) Quantification of AWC^{ON}-AWB (*G*), and AWC^{OFF}-AWB (*H*) fusion events in 1-d-old adult animals carrying either an empty vector or EFF-1 under promoters driving expression in these cells (*Pstr-1::eff-1; Pstr-2::eff-1* for AWC^{ON}–AWB fusion; *Psrsx-3::eff-1* for AWC^{OFF}–AWB fusion). These quantifications only account for specific AWC–AWB fusion, excluding AWC–AWB fusion with other neurons. Results are representative of at least two independent transgenic strains (except for the wild-type control for AWB–AWC^{OFF} fusion). N values are indicated in the graph. Error bars represent the SE of proportion.

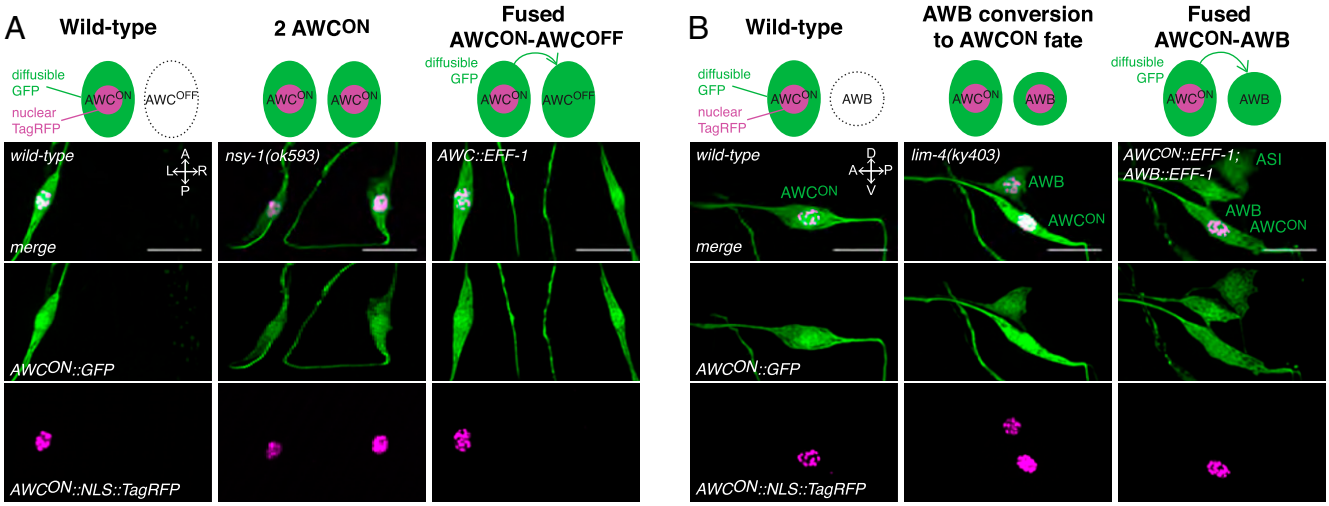

Fig. 3. Fused neurons retain the expression of neuronal cell fate markers. (*A*) (*Top*) Schematic of the assay used to assess a change in neuronal fate following fusion of AWC^{ON} and AWC^{OFF} neurons. (*Left*) A wild-type animal expresses a cytoplasmic green fluorophore (diffusible GFP) and a nuclear localized red fluorophore (nuclear TagRFP) in AWC^{ON} only. (*Middle*) A cell fate mutant animal with two AWC^{ON} neurons (*nsy-1*) expresses the same markers in both AWC neurons. (*Right*) In an animal with fused AWC^{ON}–AWC^{OFF} neurons, as evidenced by the diffusion of GFP to AWC^{OFF}, nuclear TagRFP is only visible in the AWC^{ON} neuron, suggesting that the AWC^{OFF} neuron has retained its original OFF fate. Representative confocal maximum z-projection images of the AWC neurons in wild-type animals (*Left*), *nsy-1* mutant animals (*Middle*), and animals with fused AWC^{ON}–AWC^{OFF} neurons (*Right*). (Scale bars, 10 μm.) (*B*) (*Top*) Schematic of the assay used to assess a change in neuronal fate following fusion of AWC^{ON} and AWB. For simplicity, only one AWB is represented here. (*Left*) A wild-type animal expresses a cytoplasmic green fluorophore (diffusible GFP) and a nuclear localized red fluorophore (nuclear TagRFP) in AWC^{ON} only. (*Middle*) An animal in which AWB has acquired an ON cell fate (*lim-4*) expresses these same markers in AWC^{ON} and AWB neurons. (*Right*) In an animal with fused AWC^{ON}–AWB neurons, as evidenced by the diffusion of GFP to AWB, nuclear TagRFP is only expressed in the AWC^{ON} neuron, suggesting that the AWB neuron has retained its original AWB fate. Representative confocal maximum z-projection images of the AWC^{ON} and its ipsilateral AWB neuron in wild-type animals (*Left*), *lim-4* mutant animals (*Middle*), and animals with fused AWC^{ON}–AWB neurons (*Right*) (note that, in this animal, these neurons have also undergone fusion with the ipsilateral ASI). (Scale bars, 10 μm.)

findings indicate that fusion between neurons of the same chemoattractive modality is not detrimental to the neuronal function and behavior they mediate.

However, neuronal fusion may have different consequences when the fusing partners are neurons of different modalities. To test this notion, we took advantage of the fact that AWC and AWB neurons are attractive and repulsive, respectively. We first tested individual animals with specific AWC^{OFF}–AWB fusion for their response to pentanedione, an odorant detected exclusively by the AWC^{OFF} neuron. We found that, compared to wild-type and transgenic controls, animals with fused neurons had lost chemoattraction to this odorant (Fig. 4 *A* and *E*). Importantly, this defect appeared specific to the AWC^{OFF} neuron, as the same animals were still normally attracted to butanone and benzaldehyde, both detected by the AWC^{ON} neuron (Fig. 4 *A*, *F*, and *G*). Therefore, fusion of the chemoattractive AWC^{OFF} neuron with the chemorepulsive AWB neurons compromises the chemoattraction response to pentanedione mediated by AWC^{OFF}. Next, we tested the response of the same animals to nonanone, a repellent detected by the AWB neurons (24), and found a strong defect in the response to this odorant (Fig. 4*H*). Thus, these results show that fusion between the attractive AWC^{OFF} and the repulsive AWB neurons disrupts both chemosensory responses, leaving the animals functionally compromised in their capacity to locate or move away from odorants.

To further explore this concept, we tested the effect of fusion between AWC^{ON} and AWB neurons by performing chemosensory assays with animals in which AWC^{ON} and both AWB neurons had fused (excluding all fusions with ASI neurons). We first tested animals with fused neurons for their response to butanone, which is detected exclusively by the AWC^{ON} neuron, and found that they were no longer attracted to this odorant (Fig. 4 *A* and *I*). This defect was specific to AWC^{ON}, as these animals were still attracted to pentanedione and benzaldehyde, two odorants detected by the AWC^{OFF} neuron (Fig. 4 *A*, *J*, and *K*). Therefore, fusion of the chemoattractive neuron AWC^{ON} with the chemorepulsive AWB neurons compromises the chemoattractive response to butanone mediated by the AWC^{ON} neuron. We next tested the response of these same animals to the repellent nonanone detected by the AWB neurons (Fig. 4*A*). Unlike the animals with fused AWC^{OFF}–AWB neurons, we found that animals with fused AWC^{ON}–AWB neurons still responded to this repellent, suggesting that the function of the AWB neurons was largely unaffected by fusion with AWC^{ON} (Fig. 4*L*). Taken together, these results show that fusion between a chemoattractive AWC neuron and the chemorepulsive AWB neurons affects the chemoattractive response, and can affect the chemorepulsive response depending on the specific AWC neuron involved.

Chemosensory Neurons Fuse at the Level of the Axons. The differences in the behavioral consequences of AWC^{ON}–AWC^{OFF} fusion and AWC–AWB fusion could be explained by a difference in the neuronal compartment in which the fusion events take place. The two contralateral AWC neurons only establish contact with each other in the nerve ring, where their axons form *en passant* chemical synapses (18) (Fig. 5*A*). Because cell contact is a prerequisite for cell–cell fusion, the fusion events observed between the AWC^{ON} and AWC^{OFF} neurons must occur at the level of their axons. However, the location of fusion between the AWC and AWB neurons is unknown. Importantly, an AWC neuron and its ipsilateral AWB neuron may contact each other at the level of their axons, dendrites, or sensory cilia (18, 43) (Fig. 5*B*), and fusion between these cells could therefore take place in any one of these compartments. In order to determine the location of the AWC–AWB fusion, we adopted a genetic approach and analyzed neuronal fusion in mutant animals lacking each of these three neuronal compartments. We first

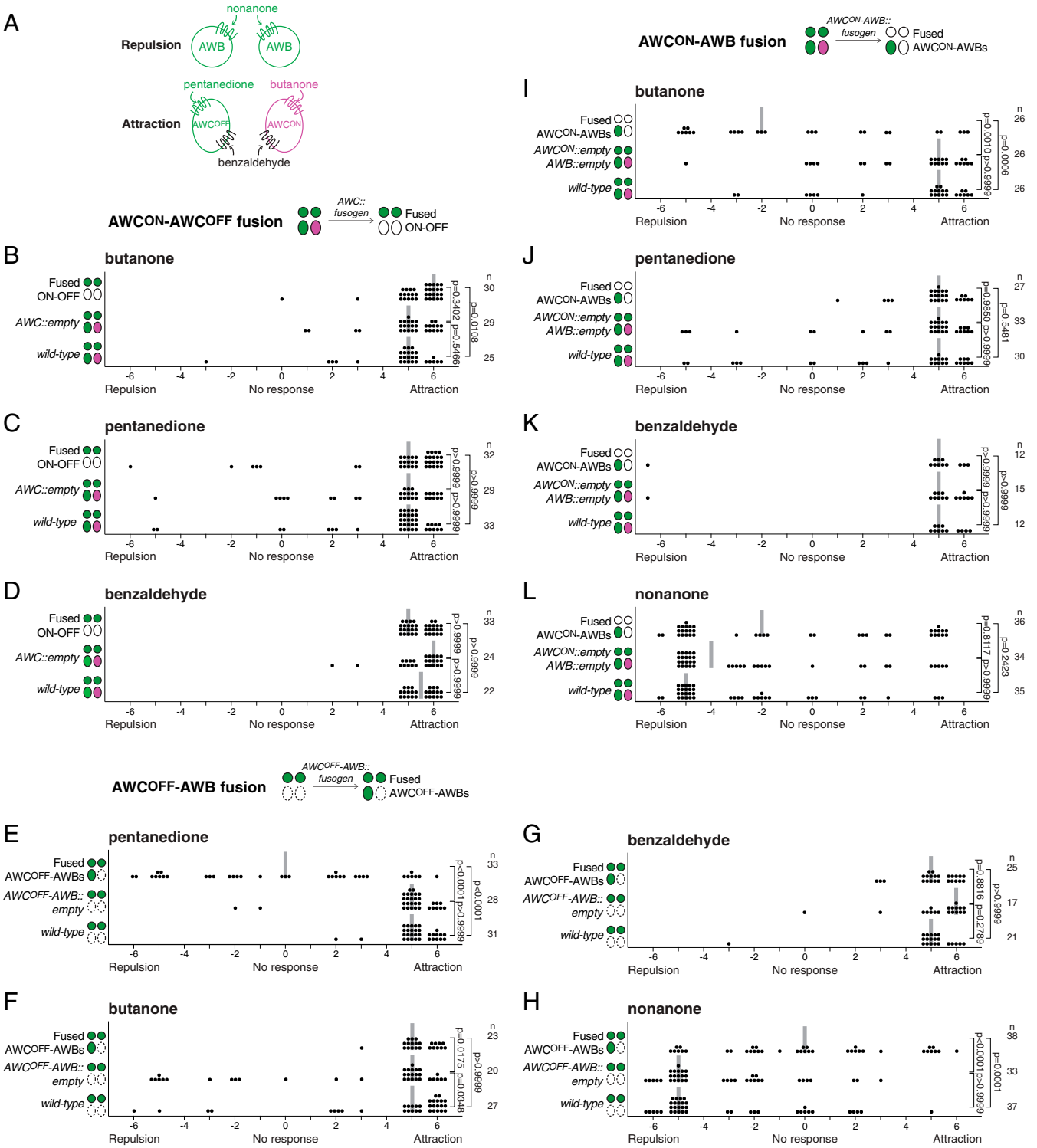

Fig. 4. Fusion between attractive neurons does not alter chemoattraction, but fusion between attractive and repulsive neurons compromises chemosensation. (*A*) Schematic representation of the odorants sensed by the attractive AWC and the repulsive AWB neurons. (*B–D*) Fusion between AWC^{ON} and AWC^{OFF} neurons does not affect the animal's response to butanone (*B*), pentanedione (*C*), or benzaldehyde (*D*). (*E–H*) Fusion between AWC^{OFF} and AWB neurons compromises the attraction response to pentanedione (*E*), and the repulsion response to nonanone (*H*), but does not affect the attraction response to butanone (*F*) or benzaldehyde (*G*). (*I–L*) Fusion between AWC^{ON} and AWB neurons compromises the attraction response to butanone (*I*), but does not affect the attraction response to pentanedione (*J*) and benzaldehyde (*K*), or the repulsion response to nonanone (*L*). In each graph, negative values represent repulsion, and positive values represent attraction to the odorant. Data are from a minimum of two independent behavioral experiments performed on different days. All animals tested had specific fusion only between the neurons of interest (*SI Appendix, Text*). Each dot represents the result of an individual assay, a vertical gray bar represents the median, and n represents the total number of animals tested for each group. Comparisons between groups were obtained using the Kruskal–Wallis statistical test.

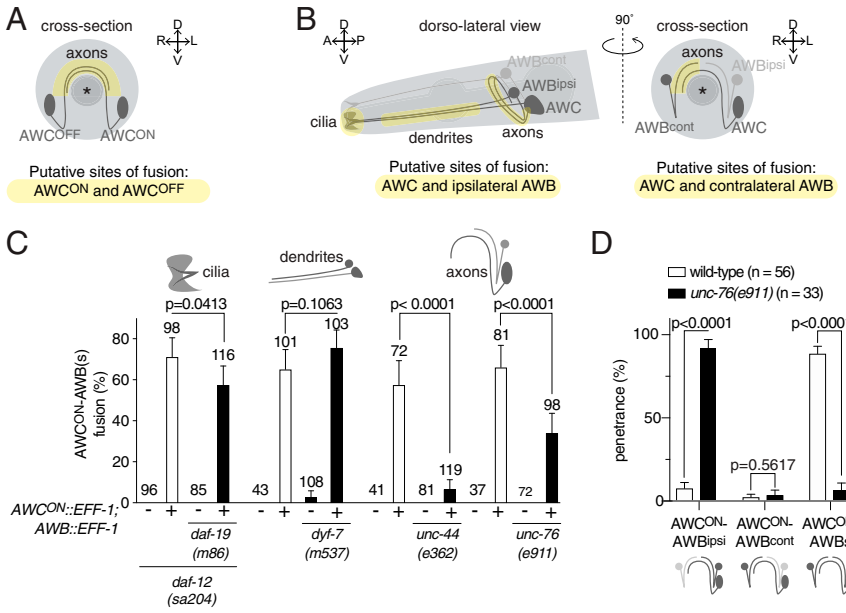

Fig. 5. Chemosensory neurons fuse at the level of the axon. (*A* and *B*) Schematic representation of the sites of contact between (*A*) AWC^{ON} and AWC^{OFF} and between (*B*) AWC and its ipsilateral AWB (*Left*) and its contralateral AWB (*Right*). Note that, while contacts between AWC^{ON} and AWC^{OFF} neurons, as well as between AWC and its contralateral AWB neuron, can only occur at the axonal level, contacts between AWC and its ipsilateral AWB neuron can occur at the level of the cilia, the dendrites, and/or the axons. (*C*) Quantification of the AWC^{ON}–AWB fusion events in mutant animals lacking cilia (*daf-19(m86)*), or dendrites (*dyf-7(m537)*), or in animals with premature axon termination (*unc-44(e362)* and *unc-76(e911)*), and their respective controls (white bars). The penetrance of fusion events is highly reduced in the absence of full-length axons. Comparisons between groups were obtained using the Wald method for comparing proportions. (*D*) Distribution of the AWC^{ON}–AWB fusion events in wild-type (white bars) and *unc-76(e911)* mutant animals (black bars), between AWC^{ON} and its ipsilateral AWB neuron, AWC^{ON} and its contralateral AWB neuron, and AWC^{ON} and the two AWB neurons. The majority of the fusion events occurring in *unc-76* mutant animals are only between AWC^{ON} and its ipsilateral AWB neuron. Comparisons between groups were obtained using the Agresti–Coull method for comparing proportions. For these analyses, all AWC^{ON}–AWB fusion events were counted, including those where fusion also involved one or two ASI neurons.

analyzed the level of fusion in the absence of cilia. DAF-19 is a key transcriptional regulator which activates the expression of genes required for normal sensory cilium formation; in its absence, all cilia are eliminated, whereas dendrites, axons, and cell bodies are largely unaffected (44, 45). When we overexpressed EFF-1 in the AWC^{ON} and AWB neurons of *daf-19* mutant animals, we observed that AWC^{ON}–AWB fusion was not suppressed (Fig. 5*C*). Following the same approach, we also found that cell–cell fusion between AWC^{OFF} and the AWB neurons did not diminish, despite the absence of cilia (*SI Appendix*, Fig. S9).

Next, we asked whether fusion between an AWC neuron and the AWB neurons takes place at the level of the dendrites. Amphid neurons in animals lacking the tectorin-like DYF-7 protein fail to develop full-length dendrites, whereas their cilia and axons develop normally (46). We therefore overexpressed EFF-1 in the AWC^{ON} and AWB neurons of *dyf-7* mutant animals, and assessed the level of neuronal fusion between these cells. Our results revealed that cell–cell fusion between AWC^{ON} and AWB neurons was unaffected in these animals, suggesting that it does not take place at the level of the dendrites (Fig. 5*C*). Similarly, we found that the level of cell–cell fusion between AWC^{OFF} and AWB neurons was not suppressed in *dyf-7* mutant animals (*SI Appendix*, Fig. S9).

Finally, we asked whether fusion between an AWC neuron and the AWB neurons takes place at the axonal level. Amphid neurons in animals lacking UNC-44/ankyrin have disrupted axons that enter the nerve ring but terminate prematurely before reaching the midline, a defect that is mainly due to the unpolarized sorting of proteins between the axons and dendrites (47, 48). When we expressed EFF-1 in the AWC^{ON} and AWB neurons of *unc-44* mutant animals, we found that fusion between these neurons was almost abolished, revealing that polarized, full-length axons are required for this fusion to occur (Fig. 5*C*). Similarly, we found that AWC^{OFF}–AWB fusion was suppressed in *unc-44* mutant animals (*SI Appendix*, Fig. S9). To determine whether the absence of fusion was due to shorter axons or to unpolarized sorting of proteins in neurites, we also analyzed AWC^{ON} and AWB fusion in animals lacking the UNC-76/FEZ-1/2 protein. In these animals, the axonal bundles are defasciculated and the axons terminate prematurely (47, 49). We found that AWC^{ON}–AWB fusion was significantly reduced, suggesting that a large proportion of fusion required fasciculating full-length axons. Thus, AWC and AWB neuronal fusion occurs at the axonal level.

A proportion of AWC^{ON}–AWB fusion events still took place in *unc-76* mutant animals (Fig. 5*C*). One possible explanation is that, in these cases, fusion occurs in the proximal section of the axon, selectively between AWC^{ON} and its ipsilateral AWB neuron (Fig. 5*B*). To test this idea, we split the fusion events into three categories: fusion between AWC^{ON} and both AWB neurons, fusion between AWC^{ON} and its contralateral AWB cell, and fusion between AWC^{ON} and its ipsilateral AWB cell. We found that, in wild-type animals, the majority of fusion events involved AWC^{ON} and both AWB neurons, whereas, in *unc-76* mutant animals, the majority of the fusion events only occurred between AWC^{ON} and its ipsilateral AWB neuron (Fig. 5*D*). This confirms that, in the absence of full-length axons, AWC^{ON} fails to fuse with the contralateral AWB neuron. Our findings also demonstrate that fusion of an AWC neuron and both AWB neurons occurs at the axonal level, and narrows down the site of fusion between the AWC neuron and its ipsilateral AWB cell to the proximal section of the axons.

Taken together, these genetic analyses reveal that, regardless of the modality of the chemosensory neurons involved, fusion takes place at the level of the axons.

Fused Attractive and Repulsive Chemosensory Neurons Respond to the Same Attractant. Both AWC and AWB neurons respond to odorant removal with an increase in calcium transients (50, 51). We therefore asked whether, following fusion of chemosensory neurons, an increase in calcium levels in one neuron following odorant removal resulted in a similar increase in the other fused neuron. To investigate this aspect, we studied the calcium response in fused AWC^{OFF}–AWB neurons, as they are activated by the removal of different odorants, pentanedione for AWC^{OFF} and nonanone for the AWB neurons (50, 51). We first expressed a calcium indicator in the AWB neurons (*Pstr-1::GCaMP*), together with EFF-1 in the AWB and AWC^{OFF} neurons (*Psrsx-3::eff-1*). We then selected individual animals with fused AWC^{OFF}–AWB

neurons based on the diffusion of the calcium indicator from AWB to AWC^{OFF} (Fig. 2*D*). As controls, we used animals expressing the calcium indicator in only the two AWB cells. We presented AWC^{OFF}–AWB fused and control animals with pentanedione, an odorant that only evokes a response in AWC^{OFF}. Fused AWC^{OFF} and AWB neurons all responded to the removal of this odorant with an increase in intracellular calcium, a response never observed in nonfused AWB control neurons (Fig. 6 *A*–*C*). These results reveal, first, that fused AWC^{OFF} cells are functional and able to respond to the removal of pentanedione and, second, that AWB neurons fused with AWC^{OFF} also respond to the removal of this odorant.

The response observed in AWB is unlikely to be due to the primary activation of these neurons by the odorant (i.e., activation by pentanedione of the odorant receptor at the cilia of AWB), given that AWB neurons do not express AWC-specific GPCR-like odorant receptors following AWC–AWB fusion (*SI Appendix*, Fig. S6). Instead, the calcium increase observed in fused AWB neurons is likely due to the diffusion of calcium transients from AWC^{OFF} to AWB through fusion pores, similar to the spreading of calcium transients through gap junctions. In agreement with this notion, we found a strong correlation in the response of fused AWC^{OFF}–ipsilateral AWB neurons, which were simultaneously recorded (Fig. 6*D*). These data suggest that the defect in the attraction to pentanedione observed in animals with fused AWC^{OFF}–AWB neurons is not due to the absence of a response of AWC^{OFF} to this odorant. Instead, the defect appears to result from the activation of both the chemoattraction and chemorepulsion circuits by AWC^{OFF} and AWB, respectively. The simultaneous activation likely generates a confounding command to the downstream interneurons and motor neurons.

It is also possible that the confounding command is caused or enhanced by the mixing of synaptic content between the two fused axons. To determine whether this could be the case, we expressed an mCherry-tagged version of the synaptic vesicle marker RAB-3 (52, 53) selectively in AWB neurons (*Pstr-1::mCherry::rab-3*), and visualized it following AWC^{ON}–AWB fusion. Remarkably, we found that RAB-3 appeared in the axon of the AWC^{ON} neuron, suggesting that mixing of synaptic vesicles between fused cells is possible, and that the fusion pores probably expanded sufficiently to allow transfer of synaptic vesicles or large macromolecules between the AWB and AWC^{ON} axons (*SI Appendix*, Fig. S10).

Discussion

Misexpression of fusogens in tightly associated *C. elegans* neurons leads to neuronal fusion and mixing of diffusible cytoplasmic content between these cells. Interestingly, compartmentalized proteins expressed in selective neurons, and used to determine cell fate, retain their original expression and localization pattern after the fusion event, suggesting that fusion does not compromise the neurons' original fate. However, neuronal fusion does compromise behavior. While fusion between the chemoattractive AWC^{ON} and AWC^{OFF} neurons does not affect chemoattraction or odorant discrimination, fusion between a chemoattractive AWC neuron and the chemorepulsive AWB neurons compromises chemosensation. Together, these results provide evidence that misexpression of fusogens in neurons compromises neuronal individuality, and suggest a model in which neuronal fusion may be detrimental to animal behavior depending on the modality of the fused neurons (Fig. 7).

The effects of fusogen overexpression in neurons could go beyond neuronal cell–cell fusion and associated behavioral defects. In *C. elegans*, fission during endocytosis and phagocytosis can be mediated by AFF-1 and EFF-1, respectively (54, 55), and EFF-1–mediated axonal fusion following injury has been shown to be regulated by the GTPase RAB-5 (56). It is therefore possible that the expression of fusogens in neurons can not only result in neuronal fusion but also impact on fission events that could affect neuronal morphology, repair, and function.

Neuronal Fusion Shortcuts Neural Circuits. Fused neurons respond to odorant removal with an increase in calcium transients, similar to nonfused wild-type chemosensory neurons. This shows that fused neurons are functional, and that the behavioral defect is not due to the absence of primary activation of these neurons by the odorant. Remarkably, however, fused neurons are coupled: upon primary activation of one of the fused neurons, changes in calcium transients are instantaneously observed in the other neuron. Coupling of fused neurons has been reported before in pseudorabies virus-infected peripheral neurons in vitro and in vivo (5, 14). Infected neurons exhibit increased and cyclic action potential firing activity, which occurs synchronously between fused cells. Interestingly, the authors propose that this synchronous activation of neurons is what causes the symptoms of peripheral pain and itching associated with pseudorabies virus infection. Here we show that fusion between chemoattractive and chemorepulsive neurons alters the chemosensory behavioral response mediated by these neurons. We suggest that this defect is due to neuronal coupling, which, upon activation by an odorant, leads to the concurrent triggering of the two different downstream circuits of attraction and repulsion, resulting in a confounding command (Fig. 7).

Conversely, we propose that fusion-mediated neuronal coupling does not compromise behavior when fused neurons are of the same modality and part of the same neural circuit. The chemoattractive AWC^{ON} and AWC^{OFF} neurons communicate with the same downstream interneurons of the neural circuit mediating attraction (50). Therefore, neuronal coupling leading to synchronous activation of these two neurons would activate the same downstream circuit, resulting in a normal attraction response (Fig. 7). This, however, is in disagreement with a previous study showing that introduction of synthetic gap junctions between AWC^{ON} and AWC^{OFF} affects chemoattraction to benzaldehyde (57). It is possible that inherent differences exist between the electrical coupling mediated by fusion versus gap junctions, making this comparison difficult. While fusion allows the flow of cytoplasmic molecules, gap junctions can interact with structural and regulatory proteins, contributing to specific intracellular signaling (1). Alternatively, given the authors expressed synthetic gap junctions in AWC neurons using the *odr-1* promoter, which is also active in the two AWB neurons, the defects in attraction to benzaldehyde they report could reflect the coupling of these four neurons together. In fact, our data indicate that coupling of the chemoattractive AWC neurons with the chemorepulsive AWB neurons results in a defect in chemoattraction.

An additional mechanism that could underlie the behavioral defects observed following AWC–AWB fusion is modification of presynaptic properties and strength. AWC neurons are glutamatergic, whereas AWB neurons are cholinergic, indicating differences in synaptic composition (50, 58). Our results with RAB-3 support the notion that fusion at the axonal level may allow the transport of full synaptic vesicles between the two axons, or the diffusion of synaptic factors and neuromodulators. This, in turn, could change how these neurons communicate with downstream interneurons. To some extent, the axons of fused neurons might therefore resemble those of hippocampal neurons, where multiple presynaptic terminals share a common vesicle superpool (59). However, despite this being a possible interpretation of our results, we currently cannot exclude that RAB-3 itself (not bound to vesicles), or its messenger RNA, diffuses to the fused neuron, or that it is expressed by the newly fused cell.

Neurotransmitter release in *C. elegans* sensory neurons is regulated by synaptic proteins in a cell-specific manner (60), and the level of specific neuromodulators at synapses can affect the behavior mediated by a given neuron (61, 62). In particular, low

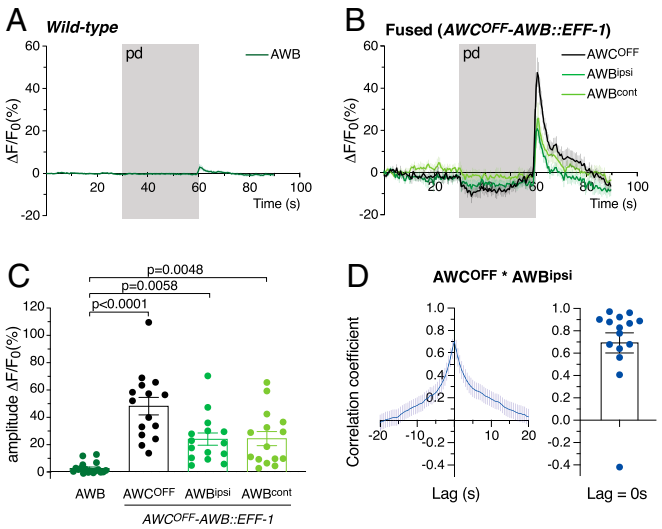

Fig. 6. Neuronal cell–cell fusion synchronizes calcium transients between fused neuronal partners. (*A* and *B*) Average calcium indicator fluorescence changes in control AWB neurons (*A*) and in AWC^{OFF}–AWB fused neurons (*B*) before, during, and after the addition of pentanedione (pd; gray bar). Whereas control AWB neurons are not activated by the removal of this AWC^{OFF}-sensed odorant, AWB neurons fused with AWC^{OFF} respond to pentanedione in synchrony with AWC^{OFF}. (*C*) Amplitude change in calcium indicator fluorescence for control AWB neurons and fused AWC^{OFF}–AWB neurons; $n = 18$ cells for control AWB, and $n = 15$ cells for each fused neuron. Error bars represent the SEM. Comparisons between groups were obtained using the one-way ANOVA. (*D*) Cross-correlation of the calcium signals between fused AWC^{OFF} and ipsilateral AWB neurons, which were simultaneously recorded. (*Left*) The average cross-correlation, and (*Right*) individual values of the peak correlation (lag = 0 s). Error bars represent the SEM. For each animal and within the same trial, fused AWC^{OFF} and the ipsilateral AWB neurons show high synchronicity ($n = 15$).

gcy-28 activity and low diacylglycerol signaling in the chemoattractive AWC^{ON} neuron results in this cell becoming repulsive to butanone (62). Moreover, changing the sign of the synapse between AWC neurons and the downstream AIY interneurons from inhibitory to excitatory compromises the attraction response to benzaldehyde (57). Fusion of the glutamatergic AWC neurons with the cholinergic AWB neurons, and eventual mixing of synaptic vesicles, could change the way in which these neurons communicate with downstream interneurons, thereby affecting the animal's response to odorants. Because AWC^{ON} and AWC^{OFF} responses to odorants are differentially affected by variations in neuromodulators levels (62), it is possible that the synaptic composition is also different in these two neurons. Synaptic mixing between AWC^{ON} and AWB, and between AWC^{OFF} and AWB, could therefore have different consequences. This would explain the disruption of AWB-mediated repulsion to nonanone by AWC^{OFF}–AWB fusion, but not by AWC^{ON}–AWB fusion.

Finally, it is also possible that fusion between two dissimilar neurons is more disruptive to the overall function and biology of the neurons than fusion between neurons of the same modality. Differences in cell composition between AWC and AWB could explain the behavioral defects observed when these cells are fused.

Fused Neurons Preserve the Expression of Neuronal Cell Fate Markers. Despite sharing diffusible cytoplasmic molecules, fused chemosensory neurons retain their original fate, as shown by the preservation of GPCR expression and localization, and the adequate activation of specific neuronal markers. This result is further confirmed by the retention of the discriminating capacity of fused AWC^{ON}–AWC^{OFF} neurons, which rely on their cell fate asymmetry to discriminate between butanone and benzaldehyde (20). However, we cannot rule out the possibility that endogenous transcription factors present in the cytoplasm may be able to diffuse through fusion pores and be imported into the nucleus of the other fused neuron. If this is the case, our results are in accordance with somatic cells being refractory to cell fate change, and the presence of a barrier for cell fate reprogramming (63–66).

An alternative interpretation of our results is that the newly formed syncytia are multinucleated neurons that, despite sharing a mixed-identity cytoplasm, retain GPCR subdomains of the plasma membrane and maintain asymmetries at the nuclear level, thereby preserving specific and diverse neuronal functions. Asymmetries at the nuclear level have been previously shown in the *C. elegans* pharyngeal muscle pm5. The *C. elegans* E/Daughterless bHLH transcription factor (CeE/DA) is expressed in some but not all of the pm5 nuclei. In one of the pm5 binucleated cells, only one of the nuclei is positive for CeE/DA (41). Nuclear heterogeneity between cells sharing a common cytoplasm has also been described in the syncytial blastoderm in *Drosophila*, in the germline of *C. elegans*, and in the skeletal muscles of mammals (reviewed in ref. 42).

Finally, maintenance of the expression of neuronal cell fate markers by fused neurons does not exclude the possibility that other cellular changes may occur. Fusion of neurons following infection with alphaherpes viruses has been shown to alter the morphology of mitochondria and reduce their motility (15). These changes are due, in part, to the electrical coupling of fused neurons, which leads to an elevated action potential firing rate and an increase in intracellular calcium. Increased calcium levels alter mitochondrial dynamics through a mechanism involving the calcium-sensitive protein Miro, thereby reducing the recruitment of kinesin-1 to mitochondria. Whether fusion-mediated electrical coupling of chemosensory neurons results in mitochondrial changes remains to be explored, together with changes in other cellular processes, such as cargo and organelle transport.

Aberrant Expression of Fusogens in Neurons Places the Nervous System at Risk. There is increasing evidence that fusogens are expressed in the nervous system in different conditions (3), such as expression of Syncytin-1 in the brain of patients with multiple sclerosis (4). Although the involvement of cell–cell fusion in this pathology remains to be explored, Syncytin-1 is not the only human endogenous retrovirus (HERV)-derived gene to be up-regulated in patients with neurological and psychiatric disorders (67, 68). Interestingly, endogenous retroviral elements are at the origin of all fusogens involved in placentation in different mammals (69), and, although most of the HERV sequences have become inactive during evolution, it is currently unknown whether other HERVs could code for fusogens in humans (70). Here we show that misexpression of fusogens in neurons leads to neuronal fusion, which can affect neural circuit connectivity and modify behavior, raising interest in studying the involvement of HERV-mediated neuronal fusion in neurological and psychiatric disorders. The extent to which viral infections expose neurons to exogenous fusogens, thereby causing them to lose their individuality and function, remains unknown. However, it is tempting to speculate that this is a highly underappreciated phenomenon with impactful medical consequences.

Materials and Methods

***C. elegans* Strains.** All strains were cultured at 20 °C following standard conditions (71) unless stated otherwise. Transgenic strains were obtained using standard microinjection techniques (72). A full list of the strains used in this study is provided in *SI Appendix*, Table S1.

Plasmids. A full list of the plasmids used in this study and the associated primers is provided in *SI Appendix*, Table S2.

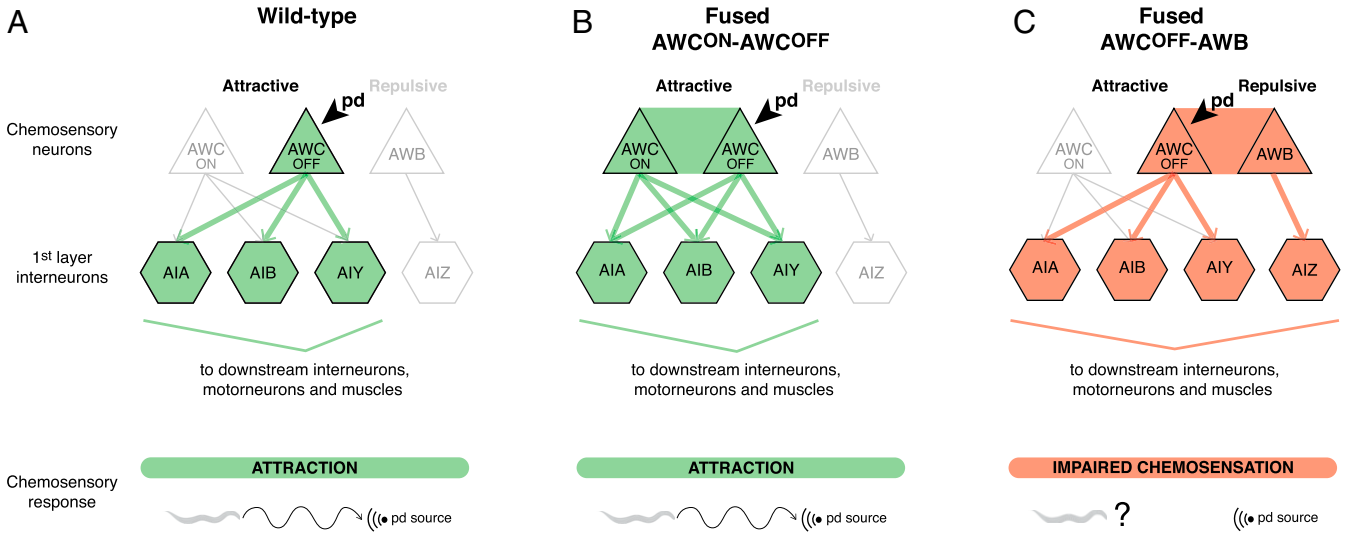

Fig. 7. Neuronal cell–cell fusion compromises neural circuit connectivity. Schematics of the connectivity between AWC and AWB chemosensory neurons and the first layer of interneurons in a wild-type animal (*A*), an animal with fused AWC^{ON}–AWC^{OFF} neurons (*B*), and an animal with fused AWC^{OFF}–AWB neurons (*C*). Arrows represent synaptic connections between neurons. Thick colored arrows represent the signaling path following detection of pentanedione (pd) by AWC^{OFF}. (*A*) In a wild-type animal, detection of pentanedione by AWC^{OFF} leads to signaling through the AIA, AIB, and AIY interneurons to the downstream interneurons, motor neurons, and muscles, resulting in chemoattraction to the source of pentanedione. (*B*) In an animal with fused AWC^{ON}–AWC^{OFF} neurons, our model predicts that detection of pentanedione by AWC^{OFF} results in the simultaneous activation of these two neurons. This results in signaling through the same downstream interneurons as in the wild-type, and therefore does not affect chemoattraction. (*C*) In an animal with fused AWC^{OFF}–AWB neurons, detection of pentanedione by AWC^{OFF} leads to the simultaneous activation of AWC^{OFF} and AWB neurons. This results in aberrant signaling through AIZ interneurons, which affects the attraction to pentanedione.

Visualization of Neuronal Cell–Cell Fusion. Animals were grown on *E. coli* OP50-seeded plates unless stated otherwise, and selected at the L4 larval stage for visualization 24 h later. The 1DOA were mounted on 3.5% agar pads in 0.05% tetramisole in M9 buffer, and visualized using a Zeiss Axio Imager Z1 microscope (Carl Zeiss AG). See *SI Appendix, Text* for details on the visualization of AWC^{ON}–AWC^{OFF}, AWC^{ON}–AWB, AWC^{OFF}–AWB, PLN–PLM, and AMsh–AWC–AWB fusion. To determine the site of fusion between AWC and AWB neurons in the absence of cilia or dendrites, or in animals with premature axon termination, fusion was visualized in *daf-19(m86) II*; *daf-12(sa204) X*, *dyf-7(m537) X*, *unc-44(e362) IV*, or *unc-76(e911) V* mutant animals (*SI Appendix, Text* and Table S1).

Kaede Diffusion Analysis of Cell–Cell Fusion. Kaede diffusion experiments were performed on L4 animals or young adults. A z-stack including both AWC neurons was obtained before, immediately after, and 30 min after conversion of Kaede in one of the neurons. Kaede was converted in only one of the AWC cell bodies, with a 405-nm laser (2% power) and 5,000 iterations, in a region of interest defined by a circle of 13 pixels diameter placed in the cytoplasm, outside of the nucleus. Calculations of the changes in intensity of converted Kaede at different time points were performed using Fiji v1.0. See *SI Appendix, Text* for more information.

Cell Fate Analyses. To study possible changes in cell fate following AWC^{ON}–AWC^{OFF} or AWC^{ON}–AWB fusion, the following neuronal markers were used: *Psrsx-3::SRSX-3::mKate2* as a marker of AWC^{OFF} fate, and *Pstr-2::STR-2::GFP* and *Pstr-2::NLS::TagRFP* as markers of AWC^{ON} fate. The *nsy-1(ok593)* mutant animals with a two-AWC^{ON} phenotype, *inx-19(ky634)* mutant animals with a two-AWC^{OFF} phenotype, and *lim-4(ky403)* mutant animals with conversion of AWB neurons into AWC^{ON} were used as controls for cell fate change. See *SI Appendix, Text* and Table S1 for details about microscopy methods and strains.

Behavior. Chemosensory assays on individual animals were performed as previously described (20, 24, 73). See *SI Appendix, Text* for details.

Calcium Imaging. Neuronal calcium responses were measured by detecting changes in the fluorescence intensity of genetically encoded Ca^{2+} indicators as previously described (50, 62, 74). Animals expressing *kyEx1423[Pstr-1::GCaMP1.0]* were used as controls. Fusion of AWC^{OFF} with the AWB neurons following expression of *Psrsx-3::eff-1* was visualized by the diffusion of GCaMP1.0 from AWB to AWC^{OFF}. Cross-correlation was analyzed using the built-in function xcorr in MATLAB. See *SI Appendix, Text* and Table S1 for detailed methods and strains.

Data Availability. All data associated with this paper are included in the paper or *SI Appendix*. All plasmids and *C. elegans* strains used in this study are listed in *SI Appendix*, and they are available upon request from the corresponding author M.A.H.

ACKNOWLEDGMENTS. We would like to thank Cori Bargmann, Sreekanth Chalasani, Chiou Fen Chuang, Oliver Hobert, Benjamin Podbilewicz, Piali Sengupta, and the *Caenorhabditis* Genetics Center (CGC) (which is funded by NIH Office of Research Infrastructure Programs [P40 OD010440]) for providing strains. We particularly thank Sreekanth Chalasani for helpful discussion on calcium imaging methods, and David Hall for discussion on amphid neurons morphology and development. We also thank past and present staff of the Queensland Brain Institute (QBI) Advanced Microscopy Facility for their help with imaging, QBI Statistician Alan Ho for his help on statistics, and past and present staff of the QBI Media Facility. We thank Denis Dupuy, Jürgen Götz, Sean Millard, and Rowan Tweedale for comments on the manuscript, and past and present members of the M.A.H. laboratory for insightful discussions. This research was supported by a Human Frontier Science Program Fellowship LT000762/2012 and an Advance Queensland Women's Academic Fund to R.G.-S., as well as National Health and Medical Research Council (NHMRC) Project Grants 1068871 and 1129367, an Australian Research Council (ARC) Discovery Project 160104359, and a NHMRC Senior Research Fellowship 1111042 to M.A.H. Imaging/analysis was performed at the QBI's Advanced Microscopy Facility using the Laser Scanning Microscope 710 META and spinning disk confocal microscopes, generously supported by the Australian Government through the ARC Linkage Infrastructure Equipment and Facilities Grant LE130100078.

1. A. B. Belousov, J. D. Fontes, Neuronal gap junctions: Making and breaking connections during development and injury. *Trends Neurosci.* **36**, 227–236 (2013).
2. S. Ramón y Cajal, Santiago Ramón y Cajal – Biographical. Nobel Media AB 2020. https://www.nobelprize.org/prizes/medicine/1906/cajal/biographical/. Accessed 11 August 2020.
3. R. Giordano-Santini, C. Linton, M. A. Hilliard, Cell-cell fusion in the nervous system: Alternative mechanisms of development, injury, and repair. *Semin. Cell Dev. Biol.* **60**, 146–154 (2016).
4. J. M. Antony *et al.*, Human endogenous retrovirus glycoprotein-mediated induction of redox reactants causes oligodendrocyte death and demyelination. *Nat. Neurosci.* **7**, 1088–1095 (2004).

5. A. E. Granstedt, J. B. Bosse, S. Y. Thiberge, L. W. Enquist, In vivo imaging of alphaherpesvirus infection reveals synchronized activity dependent on axonal sorting of viral proteins. *Proc. Natl. Acad. Sci. U.S.A.* **110**, E3516–E3525 (2013).
6. W. A. Mohler *et al*., The type I membrane protein EFF-1 is essential for developmental cell fusion. *Dev. Cell* **2**, 355–362 (2002).
7. A. Sapir *et al*., AFF-1, a FOS-1-regulated fusogen, mediates fusion of the anchor cell in *C. elegans*. *Dev. Cell* **12**, 683–698 (2007).
8. M. Oren-Suissa, D. H. Hall, M. Treinin, G. Shemer, B. Podbilewicz, The fusogen EFF-1 controls sculpting of mechanosensory dendrites. *Science* **328**, 1285–1288 (2010).
9. M. Oren-Suissa, T. Gattegno, V. Kravtsov, B. Podbilewicz, Extrinsic repair of injured dendrites as a paradigm for regeneration by fusion in *Caenorhabditis elegans*. *Genetics* **206**, 215–230 (2017).
10. A. Ghosh-Roy, Z. Wu, A. Goncharov, Y. Jin, A. D. Chisholm, Calcium and cyclic AMP promote axonal regeneration in *Caenorhabditis elegans* and require DLK-1 kinase. *J. Neurosci.* **30**, 3175–3183 (2010).
11. B. Neumann *et al*., EFF-1-mediated regenerative axonal fusion requires components of the apoptotic pathway. *Nature* **517**, 219–222 (2015).
12. V. Kravtsov, M. Oren-Suissa, B. Podbilewicz, The fusogen AFF-1 can rejuvenate the regenerative potential of adult dendritic trees by self-fusion. *Development* **144**, 2364–2374 (2017).
13. C. Procko, Y. Lu, S. Shaham, Glia delimit shape changes of sensory neuron receptive endings in *C. elegans*. *Development* **138**, 1371–1381 (2011).
14. K. M. McCarthy, D. W. Tank, L. W. Enquist, Pseudorabies virus infection alters neuronal activity and connectivity in vitro. *PLoS Pathog.* **5**, e1000640 (2009).
15. T. Kramer, L. W. Enquist, Alphaherpesvirus infection disrupts mitochondrial transport in neurons. *Cell Host Microbe* **11**, 504–514 (2012).
16. D. S. Walker, Y. L. Chew, W. R. Schafer, *Genetics of Behaviour in C. elegans* (Oxford University Press, 2017).
17. J. E. Sulston, E. Schierenberg, J. G. White, J. N. Thomson, The embryonic cell lineage of the nematode *Caenorhabditis elegans*. *Dev. Biol.* **100**, 64–119 (1983).
18. J. G. White, E. Southgate, J. N. Thomson, S. Brenner, The structure of the nervous system of the nematode *Caenorhabditis elegans*. *Philos. Trans. R. Soc. Lond. B Biol. Sci.* **314**, 1–340 (1986).
19. C. I. Bargmann, E. Hartwieg, H. R. Horvitz, Odorant-selective genes and neurons mediate olfaction in *C. elegans*. *Cell* **74**, 515–527 (1993).
20. P. D. Wes, C. I. Bargmann, *C. elegans* odour discrimination requires asymmetric diversity in olfactory neurons. *Nature* **410**, 698–701 (2001).
21. E. R. Troemel, A. Sagasti, C. I. Bargmann, Lateral signaling mediated by axon contact and calcium entry regulates asymmetric odorant receptor expression in *C. elegans*. *Cell* **99**, 387–398 (1999).
22. B. J. Lesch, A. R. Gehrke, M. L. Bulyk, C. I. Bargmann, Transcriptional regulation and stabilization of left-right neuronal identity in *C. elegans*. *Genes Dev.* **23**, 345–358 (2009).
23. S. L. Bauer Huang *et al*., Left-right olfactory asymmetry results from antagonistic functions of voltage-activated calcium channels and the Raw repeat protein OLRN-1 in *C. elegans*. *Neural Dev.* **2**, 24 (2007).
24. E. R. Troemel, B. E. Kimmel, C. I. Bargmann, Reprogramming chemotaxis responses: Sensory neurons define olfactory preferences in *C. elegans*. *Cell* **91**, 161–169 (1997).
25. J. Pérez-Vargas *et al*., Structural basis of eukaryotic cell-cell fusion. *Cell* **157**, 407–419 (2014).
26. G. Shemer *et al*., EFF-1 is sufficient to initiate and execute tissue-specific cell fusion in *C. elegans*. *Curr. Biol.* **14**, 1587–1591 (2004).
27. K. Smurova, B. Podbilewicz, Endocytosis regulates membrane localization and function of the fusogen EFF-1. *Small GTPases* **8**, 177–180 (2017).
28. O. Avinoam *et al*., Conserved eukaryotic fusogens can fuse viral envelopes to cells. *Science* **332**, 589–592 (2011).
29. R. Ando, H. Hama, M. Yamamoto-Hino, H. Mizuno, A. Miyawaki, An optical marker based on the UV-induced green-to-red photoconversion of a fluorescent protein. *Proc. Natl. Acad. Sci. U.S.A.* **99**, 12651–12656 (2002).
30. B. Neumann, K. C. Nguyen, D. H. Hall, A. Ben-Yakar, M. A. Hilliard, Axonal regeneration proceeds through specific axonal fusion in transected *C. elegans* neurons. *Dev. Dyn.* **240**, 1365–1372 (2011).
31. A. Sagasti *et al*., The CaMKII UNC-43 activates the MAPKKK NSY-1 to execute a lateral signaling decision required for asymmetric olfactory neuron fates. *Cell* **105**, 221–232 (2001).
32. B. Podbilewicz *et al*., The *C. elegans* developmental fusogen EFF-1 mediates homotypic fusion in heterologous cells and in vivo. *Dev. Cell* **11**, 471–481 (2006).
33. C. Valansi *et al*., *Arabidopsis* HAP2/GCS1 is a gamete fusion protein homologous to somatic and viral fusogens. *J. Cell Biol.* **216**, 571–581 (2017).
34. P. S. Albert, D. L. Riddle, Developmental alterations in sensory neuroanatomy of the *Caenorhabditis elegans* dauer larva. *J. Comp. Neurol.* **219**, 461–481 (1983).
35. H. M. Blau, C. P. Chiu, C. Webster, Cytoplasmic activation of human nuclear genes in stable heterocaryons. *Cell* **32**, 1171–1180 (1983).
36. H. M. Blau *et al*., Plasticity of the differentiated state. *Science* **230**, 758–766 (1985).
37. E. Schierenberg, Altered cell-division rates after laser-induced cell fusion in nematode embryos. *Dev. Biol.* **101**, 240–245 (1984).
38. B. J. Lesch, C. I. Bargmann, The homeodomain protein hmbx-1 maintains asymmetric gene expression in adult *C. elegans* olfactory neurons. *Genes Dev.* **24**, 1802–1815 (2010).
39. A. Sagasti, O. Hobert, E. R. Troemel, G. Ruvkun, C. I. Bargmann, Alternative olfactory neuron fates are specified by the LIM homeobox gene *lim-4*. *Genes Dev.* **13**, 1794–1806 (1999).
40. B. Vidal *et al*., An atlas of *Caenorhabditis elegans* chemoreceptor expression. *PLoS Biol.* **16**, e2004218 (2018).
41. M. Krause *et al*., A *C. elegans* E/Daughterless bHLH protein marks neuronal but not striated muscle development. *Development* **124**, 2179–2189 (1997).
42. G. Shemer, B. Podbilewicz, Fusomorphogenesis: Cell fusion in organ formation. *Dev. Dyn.* **218**, 30–51 (2000).
43. S. Ward, N. Thomson, J. G. White, S. Brenner, Electron microscopical reconstruction of the anterior sensory anatomy of the nematode *Caenorhabditis elegans.?*2UU. *J. Comp. Neurol.* **160**, 313–337 (1975).
44. L. A. Perkins, E. M. Hedgecock, J. N. Thomson, J. G. Culotti, Mutant sensory cilia in the nematode *Caenorhabditis elegans*. *Dev. Biol.* **117**, 456–487 (1986).
45. P. Swoboda, H. T. Adler, J. H. Thomas, The RFX-type transcription factor DAF-19 regulates sensory neuron cilium formation in *C. elegans*. *Mol. Cell* **5**, 411–421 (2000).
46. M. G. Heiman, S. Shaham, DEX-1 and DYF-7 establish sensory dendrite length by anchoring dendritic tips during cell migration. *Cell* **137**, 344–355 (2009).
47. E. M. Hedgecock, J. G. Culotti, J. N. Thomson, L. A. Perkins, Axonal guidance mutants of *Caenorhabditis elegans* identified by filling sensory neurons with fluorescein dyes. *Dev. Biol.* **111**, 158–170 (1985).
48. T. A. Maniar *et al*., UNC-33 (CRMP) and ankyrin organize microtubules and localize kinesin to polarize axon-dendrite sorting. *Nat. Neurosci.* **15**, 48–56 (2011).
49. L. Bloom, H. R. Horvitz, The *Caenorhabditis elegans* gene *unc-76* and its human homologs define a new gene family involved in axonal outgrowth and fasciculation. *Proc. Natl. Acad. Sci. U.S.A.* **94**, 3414–3419 (1997).
50. S. H. Chalasani *et al*., Dissecting a circuit for olfactory behaviour in *Caenorhabditis elegans*. *Nature* **450**, 63–70 (2007).
51. H. I. Ha *et al*., Functional organization of a neural network for aversive olfactory learning in *Caenorhabditis elegans*. *Neuron* **68**, 1173–1186 (2010).
52. G. Fischer von Mollard *et al*., rab3 is a small GTP-binding protein exclusively localized to synaptic vesicles. *Proc. Natl. Acad. Sci. U.S.A.* **87**, 1988–1992 (1990).
53. M. R. Patel *et al*., Hierarchical assembly of presynaptic components in defined *C. elegans* synapses. *Nat. Neurosci.* **9**, 1488–1498 (2006).
54. F. Soulavie, D. H. Hall, M. V. Sundaram, The AFF-1 exoplasmic fusogen is required for endocytic scission and seamless tube elongation. *Nat. Commun.* **9**, 1741 (2018).
55. P. Ghose *et al*., EFF-1 fusogen promotes phagosome sealing during cell process clearance in *Caenorhabditis elegans*. *Nat. Cell Biol.* **20**, 393–399 (2018).
56. C. Linton *et al*., Disruption of RAB-5 increases EFF-1 fusogen availability at the cell surface and promotes the regenerative axonal fusion capacity of the neuron. *J. Neurosci.* **39**, 2823–2836 (2019).
57. I. Rabinowitch, M. Chatzigeorgiou, B. Zhao, M. Treinin, W. R. Schafer, Rewiring neural circuits by the insertion of ectopic electrical synapses in transgenic *C. elegans*. *Nat. Commun.* **5**, 4442 (2014).
58. L. Pereira *et al*., A cellular and regulatory map of the cholinergic nervous system of *C. elegans*. *eLife* **4**, e12432 (2015).
59. K. Staras *et al*., A vesicle superpool spans multiple presynaptic terminals in hippocampal neurons. *Neuron* **66**, 37–44 (2010).
60. D. Ventimiglia, C. I. Bargmann, Diverse modes of synaptic signaling, regulation, and plasticity distinguish two classes of *C. elegans* glutamatergic neurons. *eLife* **6**, e31234 (2017).
61. J. D. Hawk *et al*., Integration of plasticity mechanisms within a single sensory Neuron of *C. elegans* actuates a memory. *Neuron* **97**, 356–367.e4 (2018).
62. M. Tsunozaki, S. H. Chalasani, C. I. Bargmann, A behavioral switch: cGMP and PKC signaling in olfactory neurons reverses odor preference in *C. elegans*. *Neuron* **59**, 959–971 (2008).
63. E. Kolundzic *et al*., FACT sets a barrier for cell fate reprogramming in *Caenorhabditis elegans* and human cells. *Dev. Cell* **46**, 611–626.e12 (2018).
64. S. Cheloufi *et al*., The histone chaperone CAF-1 safeguards somatic cell identity. *Nature* **528**, 218–224 (2015).
65. Y. Zhou *et al*., Bmi1 is a key epigenetic barrier to direct cardiac reprogramming. *Cell Stem Cell* **18**, 382–395 (2016).
66. C. Guo, S. A. Morris, Engineering cell identity: Establishing new gene regulatory and chromatin landscapes. *Curr. Opin. Genet. Dev.* **46**, 50–57 (2017).
67. G. Slokar, G. Hasler, Human endogenous retroviruses as pathogenic factors in the development of schizophrenia. *Front. Psychiatry* **6**, 183 (2016).
68. R. N. Douville, A. Nath, Human endogenous retroviruses and the nervous system. *Handb. Clin. Neurol.* **123**, 465–485 (2014).
69. C. Lavialle *et al*., Paleovirology of 'syncytins', retroviral env genes exapted for a role in placentation. *Philos. Trans. R. Soc. Lond. B Biol. Sci.* **368**, 20120507 (2013).
70. N. Bannert, R. Kurth, The evolutionary dynamics of human endogenous retroviral families. *Annu. Rev. Genomics Hum. Genet.* **7**, 149–173 (2006).
71. S. Brenner, The genetics of *Caenorhabditis elegans*. *Genetics* **77**, 71–94 (1974).
72. C. C. Mello, J. M. Kramer, D. Stinchcomb, V. Ambros, Efficient gene transfer in *C. elegans*: Extrachromosomal maintenance and integration of transforming sequences. *EMBO J.* **10**, 3959–3970 (1991).
73. A. C. Hart, Ed., *WormBook* (The C. elegans Research Community, 2006).
74. N. Chronis, M. Zimmer, C. I. Bargmann, Microfluidics for in vivo imaging of neuronal and behavioral activity in *Caenorhabditis elegans*. *Nat. Methods* **4**, 727–731 (2007).